Effects of nanostructured substrates on the dynamic behavior of nanobubbles

Chenliang Li,[1] A-Man Zhang,[2,*] Shi-Ping Wang,[2] and Pu Cui[2]
[1]*College of Aerospace and Civil Engineering, Harbin Engineering University, Harbin 150001, People's Republic of China*
[2]*College of Shipbuilding Engineering, Harbin Engineering University, Harbin 150001, People's Republic of China*

(Received 23 May 2019; published 15 October 2019)

The geometric structures and chemical properties of solid substrates are crucial in determining the dynamic behavior of nanobubbles. In this study, we designed a series of nanostructured substrates with alternating hydrophobic and hydrophilic domains based on the thickness and charge dependences of the hydrophobicity of graphene. We then systematically investigated the effects of these nanotrench structures on the dynamic behavior of nanobubbles using molecular-dynamics simulations. The nanotrench structures significantly enhanced the stability of bulk nanobubbles compared to homogeneous, flat graphene, and bulk nanobubble stability increased as the sizes of the hydrophilic domains increased. The mobility paths of the bulk nanobubbles were affected by the positions of the hydrophobic domains. The formation and positions of surface nanobubbles were also controlled by the properties of the nanostructured substrates; the nanobubbles were preferably located on the hydrophobic regions of the substrates. The morphologies of the surface nanobubbles depended on both the sizes of the hydrophobic regions and the degree of hydrophobicity. Under compression strain, the deformed hydrophilic domains of the solid graphene substrate prevented interactions between neighboring surface nanobubbles, resulting in stable nanobubbles. The findings provide insight into the effects of solid substrates on the dynamic behavior of nanobubbles.

DOI: 10.1103/PhysRevFluids.4.103603

I. INTRODUCTION

Nanobubbles, as nanoscopic gas bubbles, can be formed on liquid-solid interfaces (surface nanobubbles) or be suspended in solution (bulk nanobubbles) [1]. Due to the nanoscale effect, nanobubbles possess some remarkable properties, including slower rise speed, longer lifetime, and larger specific surface area compared to larger bubbles [2]. The dynamic behavior of nanobubbles attracts considerable attention since controlling the dynamic behavior of nanobubbles is significant in a wide range of applications, including protein folding, surface cleaning and antifouling, and fluid slippage [3]. The geometric structure and chemical properties of the solid substrates of surface nanobubbles play an important role in controlling the stability of the nanobubbles. Therefore, many strategies based on artificial materials have been employed to regulate the formation and stability of surface nanobubbles.

Based on experimental work, Takata *et al.* [4] found that surface nanobubbles remained stable on hydrophobic surfaces with hydrophilic domains for up to three days. Wang *et al.* [5] demonstrated that the size, position, and morphology of surface nanobubbles can be tuned by varying the surface nanostructure. He *et al.* [3] studied the formation of surface nanobubbles on two types of solid substrates, namely nanotrenches and nanopores, and they found that regulating the nanostructured

*Author to whom all correspondence should be addressed: zhangaman@hrbeu.edu.cn

substrates effectively controlled the formation and stability of surface nanobubbles. Goodwin *et al.* [6] recently demonstrated that polymer brushes can stabilize surface nanobubbles without the need for contact line pinning. These results are useful for controlling the formation, configuration, and stability of surface nanobubbles through the design of nanostructured substrates. However, experimental studies usually involve unknown factors, and it is difficult to precisely control all factors. Compared with experimental studies, theoretical simulation provides better control over the input or independent variables.

Lohse *et al.* [7] theoretically studied the growth and stability of a single surface nanobubble on a chemically heterogeneous surface using molecular-dynamics (MD) simulations. The results demonstrated that hydrophobic heterogeneity induced contact line pinning and stabilized the surface nanobubble. Liu *et al.* [8] simulated the nucleation process of surface nanobubbles on rough hydrophobic surfaces and found that solid surfaces with moderate roughness are beneficial for the formation of surface nanobubbles. Wei *et al.* [9] recently investigated the formation and stability of surface nanobubbles on chemically heterogeneous surfaces. They found that stable surface nanobubbles could exist without the contact line pinning, indicating that the stability depended on the surface hydrophobicity.

Based on these previous studies, the formation and stability of surface nanobubbles depend strongly on the properties of the solid substrate. However, due to the wide variety of substrates used in past studies, the exact relationships between substrate surface characteristics and nanobubble stability remain unclear, particularly for solid surfaces with controllable nanoscale geometries and chemical properties. Moreover, it is not known whether the properties of the solid substrate can affect the dynamic characteristics of bulk nanobubbles and multiple nanobubbles. Previous studies on surface nanobubbles have encouraged us to further investigate bulk nanobubbles and multiple nanobubbles with the goal of furthering the practical applications of nanobubbles. The graphene surface possesses hydrophobic nature, which can attract the gas molecules, resulting in spontaneous formation of nanobubbles. Some studies show that graphene can be utilized as an electrode due to its atomic thickness and its outstanding electrical and mechanical properties [10,11]. However, nanobubbles on the graphene nanoelectrode can block further proton transport, leading to a decrease in the performance of graphene electrodes [12]. Lohse *et al.* [13] also further elaborated on the nanobubble nucleation in electrochemical reactions and potential issues about the development of nanobubbles. Therefore, controlling the formation and dynamic behavior of nanobubbles by altering the hydrophobic nature and physical structure of graphene substrate is very significant to enhance the performance of a graphene device and improve the potential application of nanobubbles.

In this work, nanotrench structures with various hydrophobic properties were constructed by decorating the structures with a series of charges. The effects of these nanotrench structures on the dynamic behaviors of surface and bulk nanobubbles were investigated using MD simulations. The results suggest that the geometric structure and chemical properties of the solid substrate strongly affect the dynamic behaviors of both surface nanobubbles and bulk nanobubbles. Interestingly, the hydrophobic nature of a flat graphene surface could be altered by strain engineering, allowing two neighboring surface nanobubbles on deformed graphene to remain stable without interacting.

II. SIMULATION METHODOLOGY

All MD simulations were carried out in 5.91 nm × 31.97 nm × 10 nm simulation boxes using the GROMACS software package [14]. Three kinds of molecules were included in the simulations: graphene solid molecules, O_2 gas molecules, and liquid molecules. A united-atom model was used to represent O_2, and the liquid phase was simulated using the simple point charge (SPC) water model. The steepest-descent method was used to perform energy minimization. The configuration obtained from energy minimization was then used in *NVT* and *NPT* simulations to equilibrate the system. Finally, all simulations were carried out under the *NPT* ensemble.

We used the Lennard-Jones (LJ) 12-6 potential $U_{\mathrm{LJ}}(r_{ij}) = 4\varepsilon_{ij}(\sigma_{ij}/r_{ij})^{12} - 4\varepsilon_{ij}(\sigma_{ij}/r_{ij})^{6}$ to describe the interactions between atoms. In this equation, ε_{ij} and σ_{ij} are the interaction strength

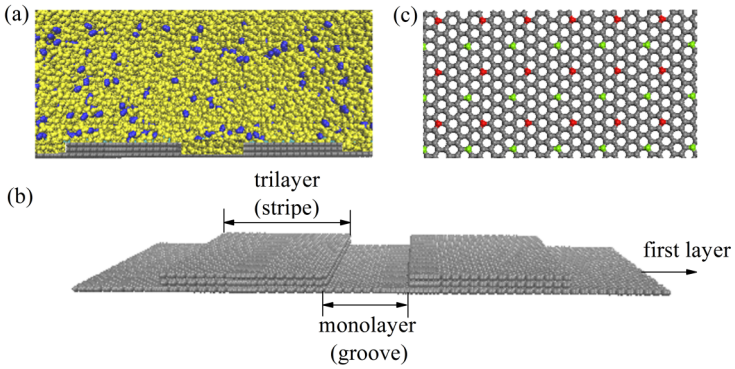

FIG. 1. (a) Initial simulation configuration (blue particles, yellow particles, and gray particles represent the gas molecules, water molecules, and graphene, respectively). (b) Nanotrench structure. (c) First-layer graphene with modified charges on the carbon atoms (the red, green, and gray balls represent carbon atoms with positive, negative, and neutral charges, respectively).

and characteristic size between atoms i and j, respectively. For carbon, $\varepsilon_{CC} = 0.439\,\mathrm{kJ/mol}$ and $\sigma_{CC} = 0.343\,\mathrm{nm}$, while for oxygen,$\varepsilon_{OO} = 0.251\,\mathrm{kJ/mol}$ and $\sigma_{OO} = 0.312$ nm. The cutoff length for the Lennard-Jones potential function was 1.5 nm. The molecular velocities and positions were updated with a time step of 2 fs, and the temperature was set at 300 K [15]. To retain a constant temperature, a V-rescale thermostat was employed to control a suitable canonical ensemble. We used periodic boundary conditions in the x, y, and z directions.

The position of the solid graphene substrate was fixed throughout the simulations, as shown in the initial configuration (0 ns) in Fig. 1(a). Above the graphene layer, the liquid molecules filled the simulation box, and the gas molecules were randomly arranged in the bulk liquid. Under the graphene layer, it is set to the vacuum region instead of the supporting substrate for the graphene layer. As a result, we can mainly consider the effects of the graphene layer on the dynamic behaviors of a nanobubble, and we ignore the effects of the supporting substrate on the simulation results. The morphological parameters of the surface nanobubbles, including contact angle, lateral size, and height, were obtained by fitting the surface nanobubble contours to circular arcs. The normalized density field was described as $\rho^*(n) = [\rho(n) - \rho_G]/[\rho_L - \rho_G]$, where ρ_L and ρ_G are the density of bulk liquid and gas, respectively [16,17]. The nanobubble contours were defined as the place at 0.5 of $\rho^*(n)$.

Solid substrates with different properties were designed to study the dynamic behavior of nanobubbles. A nanotrench structure was constructed with alternating regions (4.52 nm × 8.38 nm) of trilayer graphene (stripes) and monolayer graphene (grooves), as shown in Fig. 1(b). According to Wang *et al.* [18], the hydrophobic nature of the graphene surface can be changed by adding charges, and the size of the charge affects the degree of hydrophobicity. In this study, the carbon atoms in the first layer of graphene were assigned different charges ($q = 0.2e$, $0.4e$, $0.6e$, and $0.8e$) to produce a periodic hydrophobic/hydrophilic nanostructured surface [Fig. 1(c)]. Opposite charges of the same magnitude were imposed on the carbon atoms of first-layer graphene, and the distance between two carbon atoms with opposite charges was four times the bond length between neighboring carbon atoms (0.142 nm).

III. RESULTS AND DISCUSSION

A. Dynamic behavior of single bulk nanobubbles on the nanostructures

Previous studies have shown that when homogeneous monolayer graphene is the solid substrate, bulk nanobubbles typically exhibit zigzag motions in liquid and remain suspended in the bulk liquid

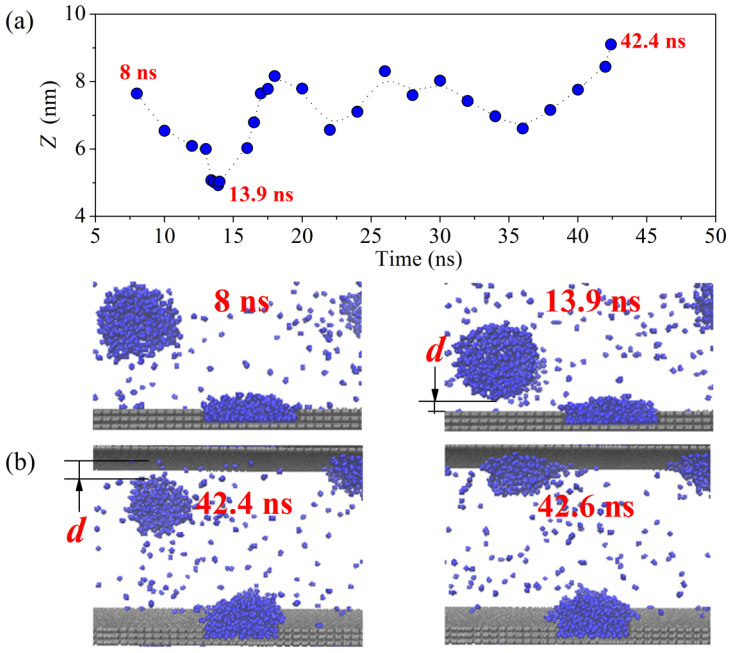

FIG. 2. (a) Position of a bulk nanobubble during the simulation of a nanotrench structure. (b) Dynamic transformation process of a bulk nanobubble into a surface nanobubble on monolayer graphene.

for less than 50 ns [2,19]. The bulk nanobubbles eventually fall onto the monolayer graphene surface because of the strong hydrophobicity of monolayer graphene. In this study, a nanotrench structure with alternating trilayer graphene and monolayer graphene was constructed as a substrate for the formation of nanobubbles. This trilayer/monolayer graphene nanostructure resulted in different bulk nanobubble dynamic behavior compared to a homogeneous monolayer graphene solid substrate. According to the experimental results of Munz *et al.* [20], trilayer graphene is more hydrophobic than monolayer graphene. Thus, the surface of trilayer graphene has a lower energy barrier compared to monolayer graphene, which is beneficial for the formation of surface nanobubbles. Surprisingly, in this study, when the bulk nanobubble was close to a trilayer graphene stripe on the trilayer/monolayer graphene substrate, the nanobubble did not locate preferentially on the trilayer graphene stripe; instead, the nanobubble rebounded off trilayer graphene [see Fig. 2(a) at 13.9 ns], indicating that the repulsive interaction between gas molecules and trilayer graphene was dominant in this case, and that the trilayer graphene surface possessed a high-energy barrier. In contrast, the attractive force was dominant on monolayer graphene; thus, surface nanobubbles formed spontaneously and occupied the monolayer graphene area. As a result, the bulk nanobubbles remained suspended in the bulk liquid.

When homogeneous monolayer graphene was located near the bulk nanobubble at 42.4 ns [Fig. 2(b)], the bulk nanobubble became a surface nanobubble on the homogeneous monolayer graphene surface. We calculated the shortest distance d between the bulk nanobubble and homogeneous monolayer graphene before the bulk nanobubble fell onto the surface. The calculated value of d (1.09 nm) was larger than the distance between the bulk nanobubble and nanostructured solid substrate when the nanobubble rebounded off the trilayer graphene stripe (0.82 nm). This indicates that monolayer graphene was more hydrophobic than trilayer graphene, and that the interaction strength between gas and monolayer graphene was higher than that between gas and trilayer graphene. This finding contradicts the experimental results of Munz *et al.* [20]. As reported previously, the polarity of the liquid medium affects the pull-off force, which scales with the degree

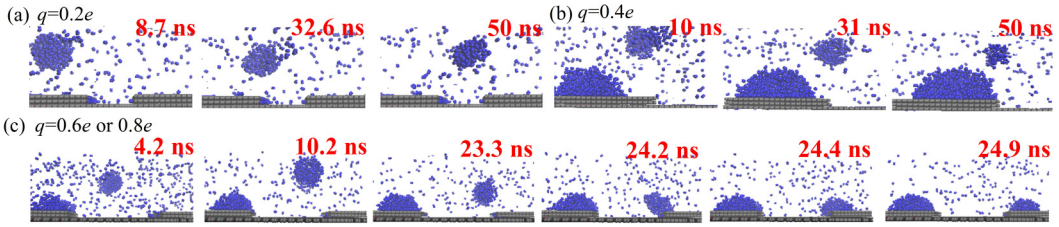

FIG. 3. Dynamic characteristics of a bulk nanobubble over nanotrench structures (groove width = 4.52 nm) with different charges: (a) $q = 0.2e$; (b) $q = 0.4e$; (c) $q = 0.6e$ or $0.8e$.

of hydrophobicity [21–24]. Due to the out-of-plane C-C interactions in the multilayer graphene system, the monolayer and trilayer graphene surfaces exhibit different properties when immersed in liquids with different polarities. The simulations in this study employed the SPC water model, resulting in a different polarity compared to experimental water. Therefore, we deduced that in the case of the SPC water model, trilayer graphene is less hydrophobic than monolayer graphene. Thus, it is necessary to further explore the effect of the water model on the hydrophobic properties of multilayer graphene in the future.

To further explore the effects of different properties of solid surfaces on the dynamic characteristics of bulk nanobubbles, the first layer of graphene in the trilayer/monolayer graphene nanostructure was decorated with a series of charges, as shown in Fig. 1(c). The polarization of the graphene surface alters the interactions between gas molecules and the solid surface, leading to changes in the hydrophobic properties of the graphene surface. When a charge of $0.2e$ is applied, monolayer graphene becomes less hydrophobic, implying that the interaction strength between gas and solid is weakened. For the nanotrench structure with $q = 0.2e$, the bulk nanobubbles remained stable and suspended in the liquid for more than 50 ns due to the weak interaction between gas and solid [Fig. 3(a)]. Monolayer graphene with $q = 0.2e$ was still more hydrophobic than trilayer graphene and attracted the bulk nanobubble, causing the bulk nanobubble to move toward monolayer graphene. Due to the lack of a three-phase contact line, the bulk nanobubble gradually shrunk in size. For $q = 0.4e$, the bulk nanobubble no longer moved toward monolayer graphene because the lower hydrophobicity of monolayer graphene with $q = 0.4e$ led to weaker interaction between gas and solid, but the bulk nanobubble was attracted to the junctions between monolayer and trilayer graphene. Moreover, the bulk nanobubble still remained suspended in the bulk liquid for over 50 ns, and a large surface nanobubble formed on the trilayer graphene stripe [Fig. 3(b)]. The weakened gas-solid interaction led to a stronger gas-gas interaction. Consequently, the gas molecules in the small bulk nanobubble were gradually absorbed into the large surface nanobubble, leading to the dissolution of the bulk nanobubble.

For $q = 0.6e$ and $0.8e$, monolayer graphene became completely hydrophilic, and the gas-solid interactions in the monolayer graphene domain were weaker than those in the trilayer graphene domain. As shown in Fig. 3(c), although the bulk nanobubble was initially located above the monolayer graphene domain, the bulk nanobubble moved toward the trilayer graphene stripe and eventually slowed down over the stripe. That is, the mobility path of the bulk nanobubble shifted based on the position of trilayer graphene. The bulk nanobubble did not merge with the surface nanobubble on the stripe. We deduced that modifying the charges of the carbon atoms in first-layer graphene caused trilayer graphene to become more hydrophobic; as a result, the gas-solid interactions of trilayer graphene were stronger than the gas-gas interactions. Consequently, the bulk nanobubbles were located preferentially on the trilayer graphene stripe rather than locating on the monolayer graphene groove or merging with a nearby surface nanobubble. The dynamic behavior of the bulk nanobubble above the nanotrench structure was similar for $q = 0.8e$; thus, only one set of simulation snapshots is shown for $q = 0.6e$ [Fig. 3(c)]. The results indicate that the properties of the solid substrate strongly influence the dynamic characteristics of bulk nanobubbles.

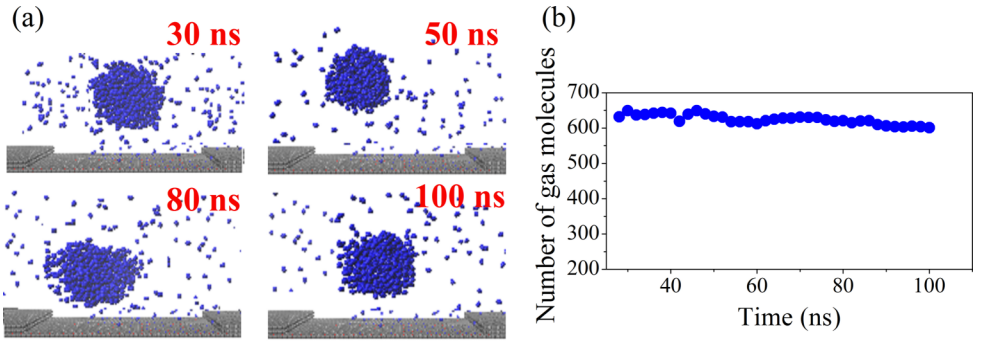

FIG. 4. (a) Dynamic characteristics of a bulk nanobubble over a nanotrench structure (groove width = 9.66 nm) with a charge of $0.8e$. (b) Variation in the number of gas molecules in the bulk nanobubble with simulation time.

In the case of $q = 0.8e$, the width of monolayer graphene in the nanotrench structure was increased to 9.66 nm. It is worth noting that the bulk nanobubble in this case remained suspended above the monolayer graphene domain for more than 100 ns without falling onto the nanostructure surface or merging with a surface nanobubble [Fig. 4(a)]. According to the calculated number of gas molecules in the bulk nanobubble, the bulk nanobubble remained stable and did not dissolve, as shown in Fig. 4(b). This result further demonstrates that the dynamic behavior of a bulk nanobubble is closely related to the size of the hydrophilic domain. It is necessary to further investigate the effects of hydrophilic domains with different sizes on the dynamic characteristics of bulk nanobubbles in the future.

B. Formation and properties of surface nanobubbles on nanostructures

The effects of the nanostructure with alternating trilayer graphene and monolayer graphene domains on the growth and formation of surface nanobubbles were also investigated. For the nanostructure without any added charge, a surface nanobubble formed spontaneously in the monolayer graphene groove due to the hydrophobic nature of monolayer graphene (Fig. 5). This again indicates that monolayer graphene was more hydrophobic than trilayer graphene in our simulations, consistent with the results presented above. Figure 5 plots the quantity of gas molecules contained in the surface nanobubble in the groove as a function of simulation time, showing the dynamic process of surface nanobubble growth. A small quantity of gas molecules began to aggregate at the edges of the groove, which should be related to the properties of joints in the monolayer/trilayer graphene pattern. These joints acted as nucleation sites for surface nanobubbles. The joint in the monolayer/trilayer graphene pattern is similar to the cleavage atomic steps on the top layer of MoS_2 or HOPG substrates in the experimental studies of Zhang *et al.* [25,26]. Their results also showed that the atomic steps can provide more favorite nucleation sites for the formation of surface nanobubbles. At 1.5 ns, the gas molecules at the edges of the groove began to merge as a result of gas-gas interactions, forming a small surface nanobubble. The small surface nanobubble was constrained in the groove and grew by gradually absorbing the surrounding gas molecules. Due to the high-energy barrier of trilayer graphene, the gas-gas interactions were stronger than the gas-solid interactions. Consequently, although the trilayer graphene surface absorbed a small quantity of gas molecules, the surface nanobubble in the groove eventually dragged these gas molecules into the groove. As shown in Fig. 5, the number of gas molecules increased suddenly from 4.2 to 4.6 ns. As a result, no gas molecules were located on the trilayer graphene stripes.

Wang *et al.* investigated the formation of surface nanobubbles on first-layer graphene with $q = 0.6e$ [3]. In this study, we evaluated the effects of graphene surfaces with different charges on the formation of surface nanobubbles. Figure 6(a) presents the morphologies of surface nanobubbles

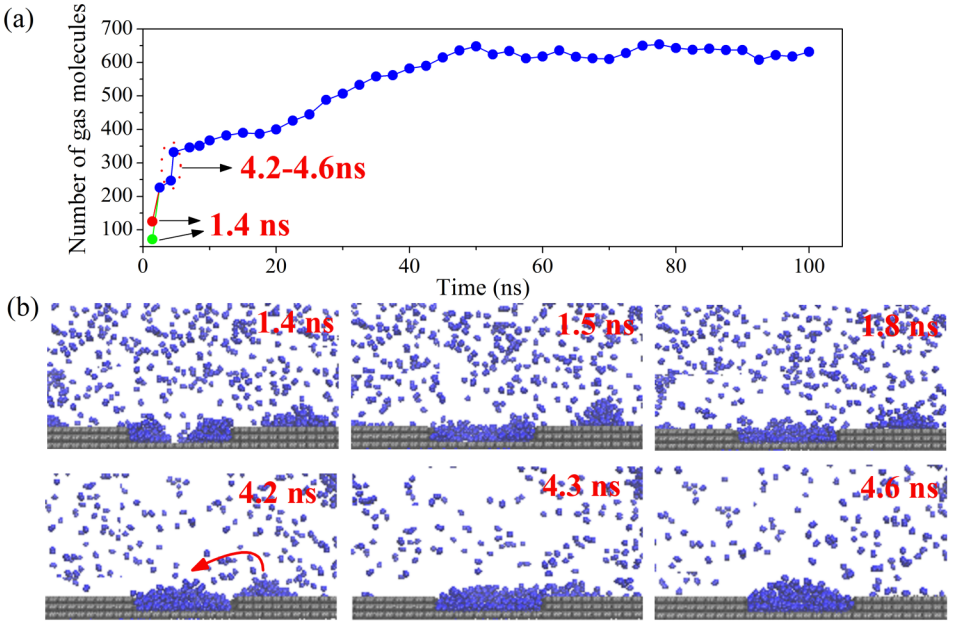

FIG. 5. (a) The quantity of gas molecules in a surface nanobubble located in a monolayer graphene groove as a function of simulation time. (b) Simulation snapshots showing the dynamic growth process of a surface nanobubble in a monolayer graphene groove.

on surfaces with various charges. For $q = 0.2e$, the joints between the monolayer and trilayer graphene domains still acted as nucleation sites and first adsorbed a small quantity of gas molecules. Subsequently, a small surface nanobubble grew gradually in the monolayer graphene groove via the adsorption of surrounding gas molecules until reaching equilibrium. When monolayer graphene was assigned a charge of $0.2e$, the grooves became less hydrophobic, suggesting that the pining force

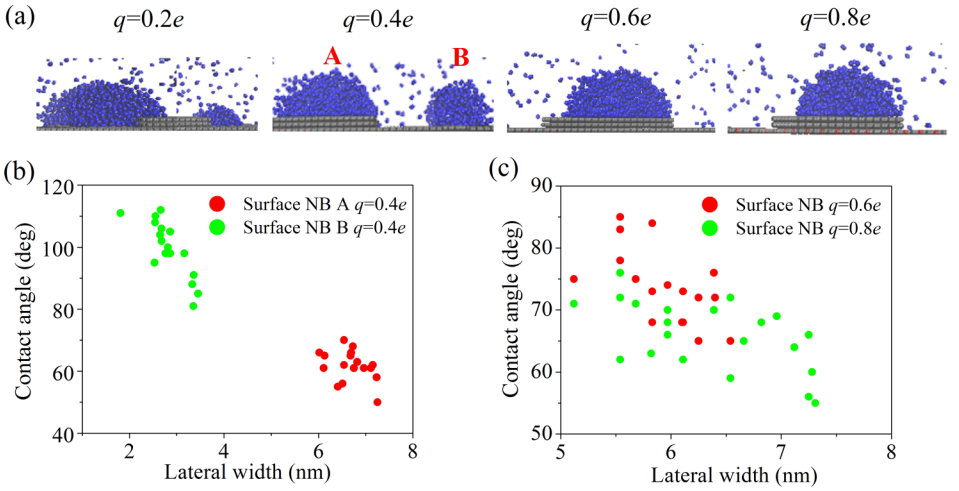

FIG. 6. (a) Surface nanobubbles formed on nanotrench surfaces with different charges. Contact angle vs lateral width for surface nanobubbles formed on trilayer graphene stripes with different charges: (b) $q = 0.4e$ and (c) $q = 0.6e$ and $0.8e$.

was reduced, and the gas-solid interaction was weakened. Consequently, the surface nanobubbles were not completely constrained to the grooves; in this case, the surface nanobubbles extended to the stripes regardless of their size, and their appearance suggested a Wenzel state [$q = 0.2e$ in Fig. 6(a)]. This indicates that the morphology of the surface nanobubble cannot be controlled by the size of the nanostructure because of the changes in the properties of the solid substrate.

When the charge q was increased to $0.4e$, the Wenzel state vanished. The changes in the hydrophilic properties of trilayer graphene under this charge caused the repulsion between gas molecules and trilayer graphene to change to attraction. As a result, the surface nanobubbles were positioned on both the stripes and the grooves [$q = 0.4e$ in Fig. 6(a)]. We also calculated the contact angles and lateral widths of the surface nanobubbles on the grooves and stripes [Fig. 6(b)]. The contact angles and lateral widths of the surface nanobubbles in the groove were clearly smaller than those of the nanobubbles on the stripe. Moreover, the lateral widths of the surface nanobubbles in the grooves were much smaller than the groove width. This may be explained by the increased hydrophilicity of monolayer graphene with $q = 0.4e$, which significantly reduced the pinning force and prevented the morphological control of the surface nanobubbles.

When the charge was $0.6e$, surface nanobubbles formed only on the stripes [$q = 0.6e$ in Fig. 6(a)]. A similar phenomenon was observed by Wang *et al.* [3], who attributed the selective adsorption of surface nanobubbles to the different hydrophobic properties of the solid surface. Thereby, we can conclude that at $q = 0.6e$, monolayer graphene became completely hydrophilic, while trilayer graphene became more hydrophobic. Consequently, trilayer graphene acted as the nucleation site where gas molecules and bulk nanobubbles were adsorbed, eventually resulting in the formation of large surface nanobubbles on the trilayer graphene stripes. Moreover, due to the hydrophilic nature of the grooves, the surface nanobubbles were constrained to the stripes and moved freely along the stripes. At $q = 0.8e$, the surface nanobubbles were again formed on the stripes but did not move freely on the nanostructure [$q = 0.8e$ in Fig. 6(a)]. We further analyzed the contact angles and lateral widths of the surface nanobubbles on the stripes for $q = 0.6e$ and $0.8e$ [Fig. 6(c)]. The contact angles and lateral widths of the surface nanobubbles on the stripes were smaller at $q = 0.8e$ compared to at $q = 0.6e$. Thus, increasing the magnitude of charge in the first layer of graphene caused trilayer graphene to become more hydrophobic. This indicates that the morphology of surface nanobubbles on trilayer graphene depends strongly on the charge in the first layer of graphene. A theoretical model [27–29] can be used to explain the morphology of surface nanobubbles on different solid substrates. The balance of forces in a surface nanobubble can be described by the Young equation $\cos\theta = (F^{\mathrm{SL}} - F^{\mathrm{SG}})/F^{\mathrm{LG}}$, where F^{LG}, F^{SG}, and F^{SL} are the liquid-gas, solid-gas, and solid-liquid boundary tensions [9], respectively. When charges are added to graphene, the hydrophobic properties of the graphene surface change, which also changes F^{SL} and F^{SG}. As a result, the morphology of surface nanobubbles is affected by the properties of the solid substrate.

C. Dynamic stability of two neighboring surface nanobubbles

Above, we discussed in detail the effects of substrate properties on the dynamic behavior of single bulk nanobubbles and surface nanobubbles. However, in most cases, multiple nanobubbles are present. Some studies have found that frictional drag can be significantly reduced because of a bubble-covering water navigator [30–34]. Therefore, the formation and stability of uniformly sized bubbles on solid surfaces is important for the application of nanobubbles in the field of drag reduction. Here, we investigated the dynamic stability and morphology of two neighboring surface nanobubbles on different nanostructured substrates. Two neighboring surface nanobubbles can remain stable with similar morphologies on two substrates: a nanotrench structure without charge and a nanotrench structure with $q \geqslant 0.6$. On the nanotrench structure without charge, the two surface nanobubbles were both positioned in the grooves [Fig. 7(a)] and remained stable without interacting. The lateral sizes of the nanobubbles were strictly confined in the grooves, resulting in nearly identical nanobubble morphologies. In contrast, for the surface with $q = 0.6e$, both surface

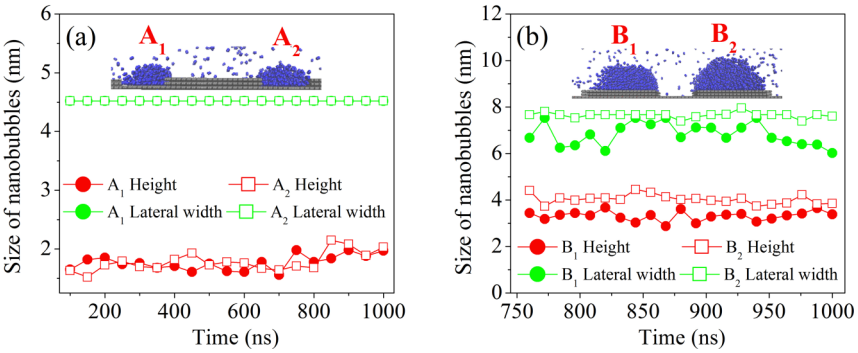

FIG. 7. Positions and morphologies of two neighboring surface nanobubbles formed on nanotrench structures without charge (a) and with $q = 0.6e$ (b).

nanobubbles were located on the stripes [Fig. 7(b)], and their morphologies were slightly different. These results suggest that the hydrophobic properties and nanostructure of the solid substrate are critical in the formation and dynamic behavior of nanobubbles and they can be used to control the nanobubble distribution and morphology on the solid substrate. Zhang *et al.* [25,26] reported that both the nanobubbles and the gas layer can form on MoS_2 or HOPG substrates, and the nanobubbles could locate on the top of the gas layer. In our studies, we only observed nanobubbles on the graphene substrate. The reason may be that (i) a lower gas supersaturation is used in our simulations; (ii) MoS_2 and HOPG possess more hydrophobicity than graphene. Their studies further indicated that the physical structure of the solid substrate is an important factor for the formation of surface nanobubbles. Based on our results, the physical structure of the substrate is closely related not only to the dynamic behavior of surface nanobubbles, but also to that of bulk nanobubbles.

We also found a new way to retain the dynamic stability of two neighboring surface nanobubbles on the homogeneous graphene surface. According to previous studies, two neighboring surface nanobubbles on flat, homogeneous monolayer graphene exhibit two types of interactions: the two nanobubbles merge into a larger nanobubble, or one nanobubble grows at the expense of the other [19]. In this study, the graphene structure between two neighboring surface nanobubbles was compressed by 50% along the Y direction [Fig. 8(a)], preventing the two nanobubbles from interacting. Figure 8(b) shows the dynamics of these two neighboring surface nanobubbles, while Fig. 8(c) shows the numbers of gas molecules in the two nanobubbles as functions of simulation time. The results reveal that the two neighboring surface nanobubbles remained stable without dissolving or interacting.

According to the theory of Henry and Laplace, the concentration of gas around a large surface nanobubble is significantly different from that around a smaller nanobubble, leading to a concentration gradient between small and large nanobubbles. As a result, small and large nanobubbles are close to each other so that they can interact finally. However, as shown in Fig. 8(d), when the distance l between two neighboring surface nanobubbles equaled the width of deformed graphene, the nanobubbles remained stable and did not interact. Moreover, the nanobubbles each moved on the surface of deformed graphene. When the structure of graphene is compressed by 50%, the interactions between atoms are enhanced, leading to changes in the properties of the graphene surface. The graphene surface becomes more hydrophilic under compressive strain, preventing the formation of a thin gas layer between two neighboring surface nanobubbles. As reported by Maheshwari *et al.* [17], this thin gas layer acts as a "tunnel" between two adjacent surface nanobubbles, which enables gas molecules to shift from one nanobubble to its adjacent one along the solid surface. In Fig. 8(b), no gas molecules are observed on the deformed graphene surface. Therefore, the two adjacent surface nanobubbles remained stable, even though a strong concentration gradient was present due to the different sizes of the two nanobubbles.

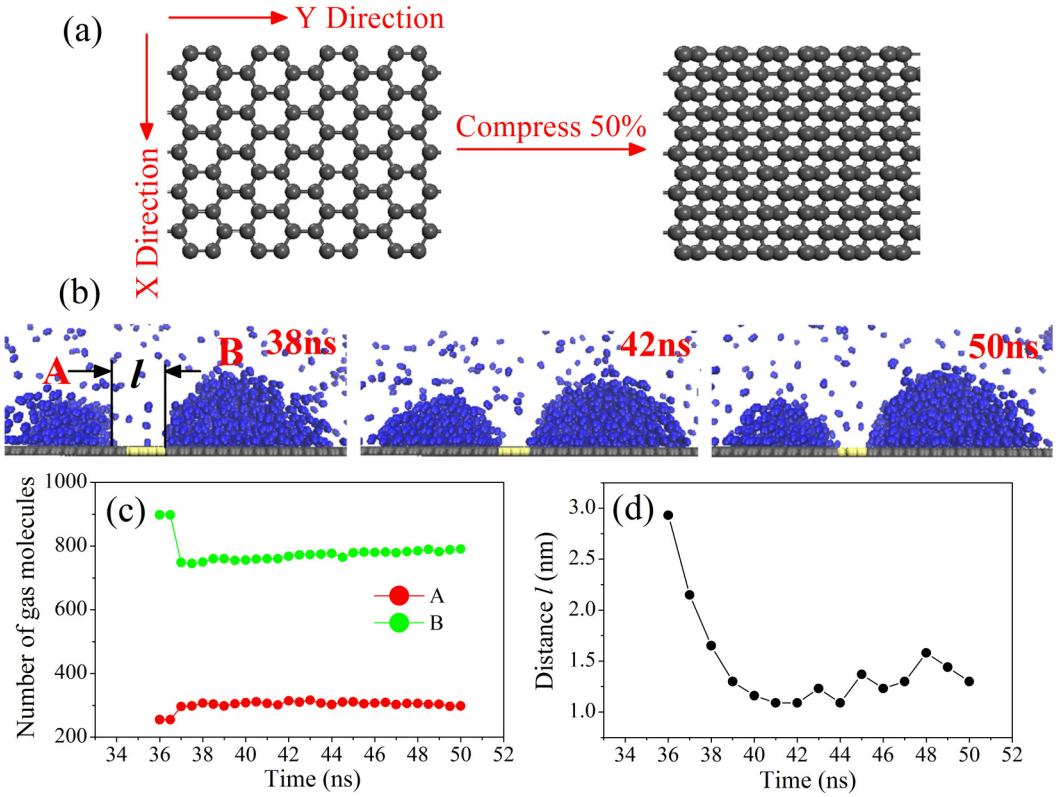

FIG. 8. (a) Original and compressed graphene structures. (b) Dynamic behavior of two neighboring surface nanobubbles on monolayer graphene under compression strain. (c) The numbers of gas molecules contained in two neighboring surface nanobubbles as functions of simulation time. (d) Distance l between two neighboring surface nanobubbles as a function of simulation time.

IV. CONCLUSIONS

Based on the thickness and charge dependences of graphene hydrophobicity, nanotrench structures with alternating hydrophobic and hydrophilic domains were designed as substrates to control the dynamic behavior of nanobubbles. The nanotrench structure obviously enhanced the stability of bulk nanobubbles, and the mobility paths of bulk nanobubbles were altered by the positions of the hydrophobic domains in the nanostructures. Bulk nanobubbles rebounded off trilayer graphene and remained suspended in bulk liquid before eventually falling onto monolayer graphene. These results indicate that monolayer graphene was more hydrophobic than trilayer graphene, which contradicts experimental results. Thus, it is necessary to further study the hydrophobic properties of multilayer graphene. The behavior of surface nanobubbles differed based on the charge added to the first layer of graphene in the nanotrench surface. For the nanotrench structure without charge, the surface nanobubbles were positioned on the monolayer graphene domains. In contrast, for $q \geqslant 0.6e$, the surface nanobubbles were located only on trilayer graphene. Moreover, the morphology of the surface nanobubbles depended on both the sizes of the hydrophobic domains and the degree of hydrophobicity. Interestingly, strain engineering caused graphene to become more hydrophilic. The hydrophilic deformed graphene domains prevented interaction between two neighboring surface nanobubbles, allowing the nanobubbles to remain stable. Altogether, the results indicate that the nanostructure and hydrophobic properties of the solid substrate are critical in determining

the dynamic behaviors of both surface nanobubbles and bulk nanobubbles. The findings provide insights into the effects of various substrate properties on the dynamic behavior of nanobubbles.

ACKNOWLEDGMENT

This work was supported by the National Natural Science Foundation of China (Grant No. 11872158).

[1] M. Zhang and J. R. T. Seddon, Nanobubble-nanoparticle interactions in bulk solutions, Langmuir **32**, 11280 (2016).
[2] C. Li, A. M. Zhang, S. Wang, and P. Cui, Formation and coalescence of nanobubbles under controlled gas concentration and species, AIP Adv. **8**, 015104 (2018).
[3] L. Wang, X. Wang, L. Wang, J. Hu, C. L. Wang, B. Zhao, X. Zhang, R. Tai, M. He, L. Chen, and L. Zhang, Formation of surface nanobubbles on nanostructured substrates, Nanoscale **9**, 1078 (2017).
[4] T. Nishiyama, K. Takahashi, T. lkuta, Y. Yamada, and Y. Takata, Hydrophilic domains enhance nanobubble stability, Chem. Phys. Chem. **17**, 1500 (2016).
[5] Y. Wang, X. Li, S. Ren, H. T. Alem, L. Yang, and D. Lohse, Entrapment of interfacial nanobubbles on nano-structured surfaces, Soft Matter **13**, 5381 (2017).
[6] D. S. Bull, N. Nelson, D. Konetski, C. N. Bowman, D. K. Schwartz, and A. P. Goodwin, Contact line pinning is not required for nanobubble stability on copolymer brushes, J. Phys. Chem. Lett. **9**, 4239 (2018).
[7] S. Maheshwari, M. Hoef, X. Zhang, and D. Lohse, Stability of surface nanobubbles: A molecular dynamics study, Langmuir **32**, 11116 (2016).
[8] Y. Liu and X. Zhang, Molecular dynamics simulation of nanobubble nucleation on rough surfaces, J. Chem. Phys. **146**, 164704 (2017).
[9] J. Wei, X. Zhang, F. Song, and Y. Shao, Nanobubbles in confined solution: Generation, contact angle, and stability, J. Chem. Phys. **148**, 064704 (2018).
[10] D. S. L. Abergel, V. Apalkov, J. Berashevich, K. Ziegler, and T. Chakraborty, Properties of graphene: A theoretical perspective, Adv. Phys. **59**, 261 (2010).
[11] D. Shin, J. B. Park, Y. Kim, S. J. Kim, J. H. Kang, B. Lee, S. P. Cho, B. H. Hong, and K. S. Novoselov, Growth dynamics and gas transport mechanism of nanobubbles in graphene liquid cells, Nat. Commun. **6**, 6068 (2014).
[12] P. E. Sharel, Y. R. Kim, D. Perry, C. L. Bentley, and P. R. Unwin, Nanoscale electrocatalysis of hydrazine electro-oxidation at blistered graphite electrodes, ACS Appl. Mater. Interfaces **8**, 30458 (2016).
[13] D. Lohse and X. Zhang, Surface nanobubbles and nanodroplets, Rev. Mod. Phys. **87**, 981 (2015).
[14] B. Hess, C. Kutzner, D. Van der Spoel, and E. Lindahl, GROMACS 4: Algorithms for highly efficient, load-balanced, and scalable molecular simulation, J. Chem. Theor. Comput. **4**, 435 (2008).
[15] G. Menzl, M. A. Gonzalez, P. Geiger, F. Caupin, J. L. F. Abascal, C. Valeriani, and C. Dellago, Molecular mechanism for cavitation in water under tension, Proc. Natl. Acad. Sci. USA **113**, 13582 (2016).
[16] J. Wei, X. Zhang, and F. Song, Deformation of surface nanobubbles induced by substrate hydrophobicity, Langmuir **32**, 13003 (2016).
[17] S. Maheshwari, M. van der Hoef, J. R. Rodriguez, and D. Lohse, Leakiness of pinned neighboring surface nanobubbles induced by strong gas-surface interaction, ACS Nano **12**, 2603 (2018).
[18] S. Wang, Y. S. Tu, R. Z. Wan, and H. P. Fang, Effects of surface dipole lengths on evaporation of tiny water aggregation, Commun. Theor. Phys. **59**, 623 (2013).
[19] C. L. Li, S. P. Wang, A. M. Zhang, and Y. L. Liu, Dynamic behavior of two neighboring nanobubbles induced by various gas-liquid-solid interaction, Phys. Rev. Fluids **3**, 123604 (2018).
[20] M. Munz, C. E. Giusca, R. L. Myers-Ward, D. K. Gaskill, and O. Kazakova, Thickness-dependent hydrophobicity of epitaxial graphene, ACS Nano **9**, 8401 (2015).

[21] S. Clear and P. Nealey, Chemical force microscopy study of adhesion and friction between surfaces functionalized with self-assembled monolayers and immersed in solvents, J. Colloid Interface Sci. **213**, 238 (1999).
[22] S. Gourianova, N. Willenbacher, and M. Kutschera, Chemical force microscopy study of adhesive properties of polypropylene films: Influence of surface polarity and medium, Langmuir **21**, 5429 (2005).
[23] H. J. Butt, B. Cappella, and M. Kappl, Force measurements with the atomic force microscope: Technique, interpretation and applications, Surf. Sci. Rep. **59**, 1 (2005).
[24] E. Kokkoli and C. Zukoski, Effect of solvents on interactions between hydrophobic self-assembled monolayers, J. Colloid Interface Sci. **209**, 60 (1999).
[25] X. H. Zhang, X. Zhang, J. Sun, Z. Zhang, G. Li, G. Li, H. Fang, X. Xiao, X. Zeng, and J. Hu, Detection of novel gaseous states at the highly oriented pyrolytic graphite-water interface, Langmuir **23**, 1778 (2007).
[26] X. Zhang and N. Maeda, Interfacial gaseous states on crystalline surface, J. Phys. Chem. C **115**, 736 (2011).
[27] B. Koch, A. Amirfazli, and J. Elliott, Modeling and measurement of contact angle hysteresis on textured high-contact-angle surfaces, J. Phys. Chem. C **118**, 18554 (2014).
[28] N. Shardt and J. Elliott, Thermodynamic study of the role of interface curvature on multicomponent vapor-liquid phase equilibrium, J. Phys. Chem. A **120**, 2194 (2016).
[29] L. Zargarzadeh and J. Elliott, Thermodynamics of surface nanobubbles, Langmuir **32**, 11309 (2016).
[30] B. R. Elbing, S. Makiharju, A. Wiggins, M. Perlin, D. R. Dowling, and S. L. Ceccio, On the scaling of air layer drag reduction, J. Fluid Mech. **717**, 484 (2013).
[31] B. R. Elbing, E. S. Winkel, K. A. Lay, S. L. Ceccio, D. R. Dowling, and M. Perlin, Bubble-induced skin-friction drag reduction and the abrupt transition to air-layer drag reduction, J. Fluid Mech. **612**, 201 (2008).
[32] Y. Murai, H. Oiwa, and Y. Takeda, Frictional drag reduction in bubbly Couette-Taylor flow, Phys. Fluids **20**, 034101 (2008).
[33] W. C. Sanders, E. S. Winkel, D. R. Dowling, M. Perlin, and S. L. Ceccio, Bubble friction drag reduction in a high-Reynolds-number flat-plate turbulent boundary layer, J. Fluid Mech. **552**, 353 (2006).
[34] T. H. van den Berg, S. Luther, D. P. Lathrop, and D. Lohse, Drag Reduction in Bubbly Taylor-Couette Turbulence, Phys. Rev. Lett. **94**, 044501 (2005).